ELSEVIER

Journal of Chromatography A, 852 (1999) 105–115

JOURNAL OF CHROMATOGRAPHY A

New ligand, *N*-(2-pyridylmethyl)aminoacetate, for use in the immobilised metal ion affinity chromatographic separation of proteins

Hassan Chaouk[1], Milton T.W. Hearn*

Centre for Bioprocess Technology, Department of Biochemistry and Molecular Biology, Monash University, Clayton, Victoria 3168, Australia

Abstract

A new chelating compound has been developed for use in the immobilised metal ion affinity chromatographic separation of proteins. The tridentate ligand, sodium *N*-(2-pyridylmethyl)aminoacetate (carbpyr), **1**, was prepared via a one-step synthesis from 2-picolylamine, **3** and then immobilised onto Sepharose CL-4B through the epoxide coupling procedure. The binding behaviour of the resulting IMAC sorbent, following chelation with Cu^{2+} ions to a density of 152 μmol Cu^{2+} ions/g gel was characterised by frontal analysis experiments using horse heart myoglobin (HMYO) at pH 7.0 and pH 9.0. From the derived isotherms, the adsorption capacity, q_m, for the binding of HMYO to immobilised Cu^{2+}–*N*-(2-pyridylmethyl)aminoacetate (im-Cu^{2+}–carbpyr)-Sepharose CL-4B at these pH values was found to be 1.92 and 1.91 μmol/g sorbent, respectively, whilst the dissociation constants K_D were $0.0092 \cdot 10^{-6}$ *M* and $0.0062 \cdot 10^{-6}$ *M* at pH 7.0 and pH 9.0, respectively, indicating that the HMYO–im-Cu^{2+}–*N*-(2-pyridylmethyl)aminoacetate complex was more stable under alkaline conditions, although the binding capacity in terms of μmol protein/g gel remained essentially unchanged. The selectivity features of the im-Cu^{2+}–carbpyr-Sepharose CL-4B sorbent were further characterised in terms of the binding properties with several human serum proteins at pH 5.0, pH 7.0 and pH 9.0.

Keywords: Pyridylmethylaminoacetate ligands; Immobilised metal affinity chromatography; Affinity sorbents; Proteins

1. Introduction

Immobilised metal ion affinity chromatography (IMAC) is a versatile separation procedure that exploits differences in the affinities exhibited by many biopolymers for metal ions. The technique involves the chelation of a suitable metal ion onto a solid support matrix, whose surface has previously been chemically modified with a polydentating ligand. The resulting metal ion chelating ligate then has the potential to coordinate with electron donor group(s) resident on the surface of the interacting protein [1–4]. The separation selectivity is then achieved on the basis of differences in the thermodynamic stabilities of the protein–metal ion chelating ligate complexes. Proteins which form adsorption complexes of low stability will be eluted first, whilst proteins that form more stable complexes will be eluted later. As the differences in the equilibrium association constants increase for the respective

*Corresponding author. Fax: +61-3-9905-5882.

E-mail address: milton.hearn@med.monash.edu.au (M.T.W. Hearn)

[1]Present address: CSIRO Division of Molecular Sciences, Clayton, Victoria 3168, Australia.

0021-9673/99/$ – see front matter
PII: S0021-9673(99)00368-4

protein–metal ion chelating ligate coordination complexes, then higher will be the resolution so obtained. Consequently, the amino acid composition, the surface distribution of particular amino acid residues, as well as the conformation of the protein in solution and on docking with the IMAC ligate all play important roles in determining the affinity of a protein for the immobilised metal ion–chelate complex in a particular IMAC system. As a result, proteins with very similar properties with respect to charge, molecular size and amino acid composition, but with differences in their tertiary structures or surface array of specific amino acid residues may be resolved [2–4].

Much of the research interest into the use of IMAC over the past 20 years has revolved around the application of borderline first row, transition metal ions, such as Cu^{2+}, Zn^{2+} and Ni^{2+}. These metal ions demonstrate intermediate metal ion stability constants, e.g., log β values between 5 and 10, for both aromatic and aliphatic amines, as well as carboxylate groups [5,6]. Several of the commonly available tridentating chelates, which exhibit these binding properties with M^{2+} ions, are relatively inexpensive compounds and can be chemically immobilised onto a range of support materials by straightforward procedures. It is perhaps for these latter reasons, rather than the magnitude of its corresponding log β value, that iminodiacetic acid (IDA, **2** Fig. 1) has come to represent the principle chelating ligand in many IMAC investigations [1–4]. Thus, despite the relatively modest metal ion stability constants exhibited with most borderline metal ions [2,4,6], a preference for immobilised M^{2+}–IDA systems has been shown by many investigators, not only in terms of the different metal ions used, but also in terms of the selectivity changes that can be achieved with different adsorption and elution buffer systems [7–10].

Illustrative uses of M^{2+}–IDA-based IMAC systems include the purification of α-amylases [11] from germinated wheat with immobilised Cu^{2+}–IDA; clotting factor VII [12] or α_1-thiol proteinases [13] from human plasma with immobilised Zn^{2+}–IDA; and α-D-mannosidases [14] from monkey brain with immobilised Co^{2+}–IDA. As a logical extension of the application of IDA-based IMAC procedures, analogues of IDA, such as immobilised Ca^{2+}–carboxymethylated aspartic acid (Ca^{2+}–CM-ASP) [15,16] or *cis*- and *trans*-*N*-(carboxymethyl)-4-amino-L-proline [17] have been employed for the purification of α_1-glycoproteins and other proteins from human serum. Purification of recombinant proteins with immobilised Ni^{2+}–nitrilotriacetic acid (Ni^{2+}–NTA) [18–20], an additional analogue of IDA, has also gained popularity by relying on the incorporation at the gene level of a polynucleotide sequence corresponding to a polyhistidine peptide, typically hexa-His, thus engendering an affinity tail to the protein for subsequent binding to the Ni^{2+}–NTA ligate.

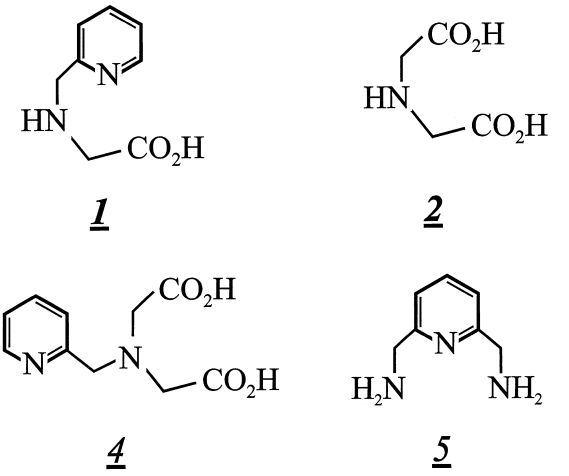

Fig. 1. Structural relationship of the ligand *N*-(2-pyridylmethyl)aminoacetic acid **1** to iminodiacetic acid **2**, *N*-(2-pyridylmethyl)amino-bis-acetic acid **3**, and 2,6-diaminomethylpyridine, **5**.

Alternative means of affecting protein selectivity in IMAC systems can thus be achieved through variation in the structure of the chelating ligate. In recent years, however, only a handful of new IMAC chelating ligates has been introduced. In most cases, these IMAC ligates are conformationally unconstrained and include (i) bidentate chelators, such as salicylaldehyde, aminohydroxamic acid (AHM) [21] or 8-hydroxy-quinoline (8-HQ) [3,22]; (ii) *ortho*-phosphoserine (OPS) [23], which can chelate many hard Lewis metal ion (e.g., Fe^{3+}, Al^{3+}, Ca^{2+} or Yb^{3+}) due to the participation of the phosphate group, and other tridentating ligates, such as dipicolylamine (DPA) [24], *cis*- or *trans*-carboxymethylproline [17]; (iii) tetradentate ligands, in-

cluding NTA, which have higher affinities for M^{2+} ions than IDA due to their quadradentate nature but exhibit lower protein binding association constants due to the loss of one coordination site compared to the IDA-type tridentate ligates [17–20]; and (iv) pentadentate ligands, such as *N*,*N*,*N*′-tris-(carboxymethyl)ethylenediamine (TEA) [24], which can coordinate metal ions via two nitrogen atoms of secondary amino groups and three oxygen atoms from the three carboxylic groups. Polydentating nitrogen ligands based on 1,4,7-triazacyclononane (Tacn) macrocyclic structures [25] or tetraethylenepentamine (TEPA) [15,24] have also been used for IMAC applications with proteins, since these systems exhibit much higher metal ion stability constants, e.g., log β values >15 for Tacn systems, as well as novel selectivity dependencies on pH and ionic strength. Significant leakage of metal ions has also been observed with im-M^{n+}–IDA complexes when relatively mild elution conditions have been used in the chromatographic process [2,4,17]. Besides the issue of selectivity modulation, the requirement to achieve increased metal ion stability constants compared to the corresponding IDA systems has provided an additional motivation for the development of new chelating ligates.

The studies described in this paper have focused on the synthesis and characterisation of a new tridentating chelate, sodium *N*-(2-pyridylmethyl)aminoacetate (carbpyr) (**1**, Fig. 1). This new chelate has then been used in the IMAC analysis and separation of proteins. The adsorption properties of the resulting IMAC sorbent, following chelation with Cu^{2+} ions, were characterised with horse heart myoglobin (HMYO) using frontal analysis experiments under neutral and alkaline pH conditions. In addition, the binding behaviour has been examined with several human serum proteins.

2. Materials and methods

2.1. Chromatographic methods and equipment

Sepharose CL-4B (Lot No. RM 15421) was obtained from Pharmacia Bioprocess (Uppsala, Sweden) and HMYO (95–100%, Lot Nos. 61H7105 and 61H7106) from Sigma (St. Louis, MO, USA). All experiments were carried out at room temperature with a fast protein liquid chromatography (FPLC) system (Pharmacia Biotech, Uppsala, Sweden) comprising two Model P-500 high-precision pumps, a Model P-1 peristaltic pump, a Model UV-1 single-path wavelength monitor and controller and chart recorder.

2.2. Frontal analysis experiments

The IMAC gel was packed into glass HR 5/2 columns (Pharmacia) of 5 mm I.D. To saturate the *N*-(2-pyridylmethyl)aminoacetate-Sepharose CL-4B gel with Cu^{2+} ions, each packed chromatographic bed was initially equilibrated by washing (per ml of gel) with a minimum of 20 ml of a solution of 50 m*M* ethylenediaminetetraacetic acid (EDTA) (disodium salt)–500 m*M* NaCl and 12 ml of water, and then sequentially with 15 ml of a solution of 50 m*M* $Cu(NO_3)_2$–500 m*M* NaCl, 15 ml of water, 5 ml of a solution of 100 m*M* acetic acid (pH 4)–500 m*M* NaCl and finally with 20 ml of water. All the solutions were delivered via the peristaltic pump at a flow-rate of 0.85 ml/min. The columns were then equilibrated with 20 ml of 20 m*M* sodium phosphate buffer–500 m*M* NaCl at pH 7.0 or pH 9.0 through a high-precision pump at a flow-rate of 0.2 ml/min. HMYO was dissolved in the equilibration buffer (20 m*M* sodium phosphate containing 500 m*M* NaCl, pH 7.0 or pH 9.0) and the protein concentration in the column effluent determined from the UV absorbance at 280 nm. For the frontal breakthrough studies, the protein solution was loaded onto the column via a second high-precision pump at a flow-rate of 0.2 ml/min using the equipment layout schematically shown in Fig. 2. In order to determine the value of the breakthrough volume (V_e) and hence the adsorbate concentration (q) at the breakthrough point at $V_e = 0.5$, it was necessary to solve the integral of the area under the breakthrough curve. This was performed by a computer program written in QBASIC which inter-linked the relationship between V_e and the initial adsorbate concentration, C, such that

$$V_e = \frac{1}{C}\int_0^C [V \partial C_{1-n}] \quad (1)$$

$$q = C\,x\,(V_e - V_0) \quad (2)$$

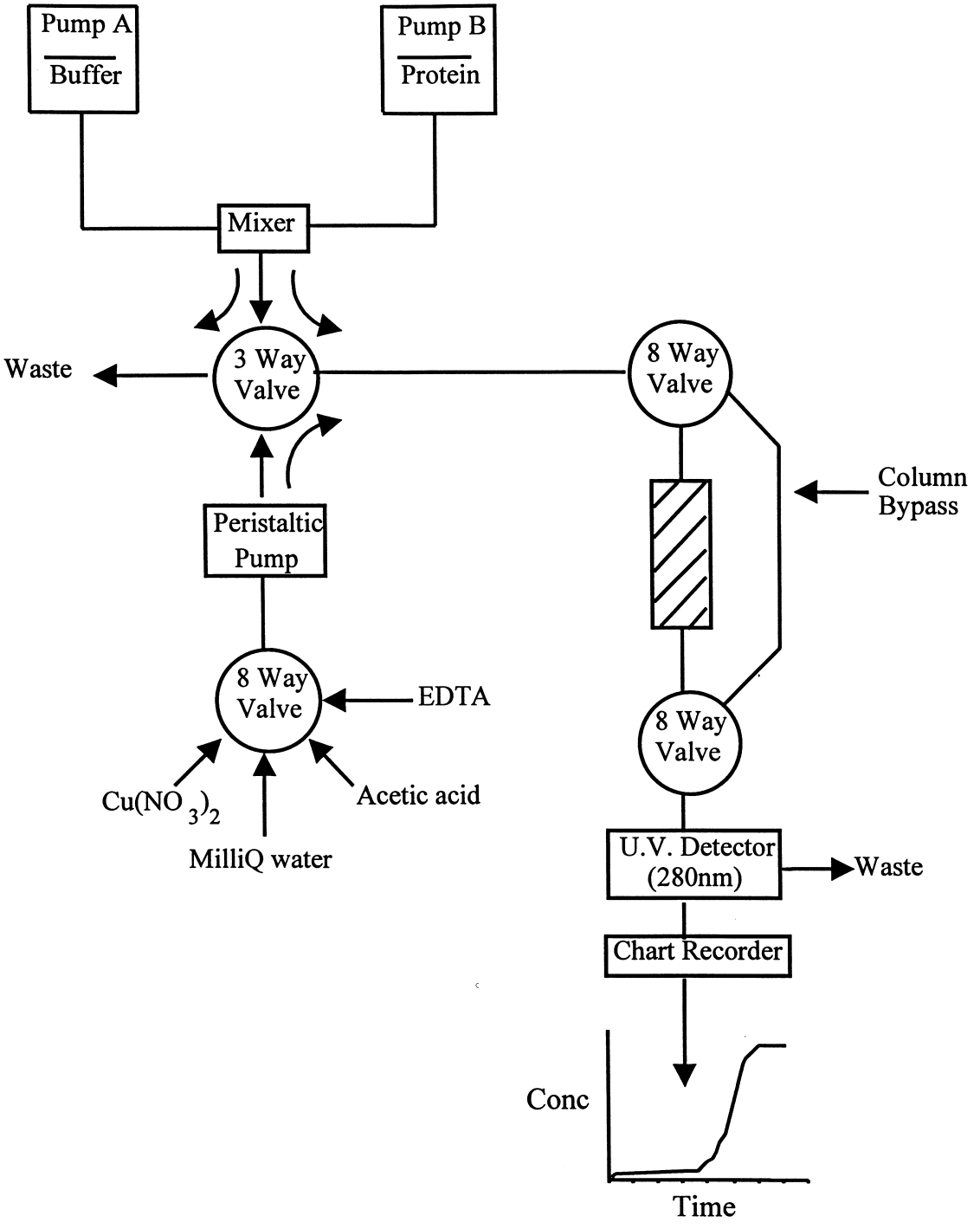

Fig. 2. Schematic showing the equipment layout for the frontal and zonal elution experiments carried out to characterise the adsorption behaviour of the immobilised Cu^{2+}–*N*-(2-pyridylmethyl)aminoacetate-Sepharose CL-4B sorbent with horse heart myoglobin (HMYO) and human serum proteins.

where C_{1-n} corresponds to momentary adsorbate concentration in the column outlet, V is the momentary volume, V_e the elution volume of the adsorbate and V_0 is the dead volume of the chromatographic system. The breakthrough curves from the frontal analysis experiments were analysed according to an adaptation of the methods reported by Nichol et al. [26] and Anspach et al. [27,28]. The average adsorbate concentration, q, at the midpoint of the breakthrough curve can be related to the initial adsorbate concentrate, C, at equilibrium through the expression:

$$\frac{C}{q} = \frac{1}{q_m} \cdot C + \frac{K_D}{q_m} \quad (3)$$

where q_m is the maximum adsorbate concentrate and K_D is the dissociation constant. Linear regression analysis and curve fitting of the experimental data were carried out as described previously [17,27–29], generating the double reciprocal, semi-reciprocal and Scatchard plots from the experimental adsorption results.

2.3. Screening of human serum proteins with the immobilised metal affinity sorbent

Plasma protein fractions (batch CA64), free of cryoprecipitant and depleted of fibrinogen, were supplied by CSL (Melbourne, Australia). These fractions were kept in liquid form at a protein concentration of 50 mg/ml in 8% (v/v) ethanol and stored frozen at −25°C in 5-ml ampoules until required for IMAC screening. Aliquots of the thawed serum protein solution were then desalted using Sephadex PD10 columns (5×1.5 cm I.D.) (Pharmacia Biotech). Desalted protein samples (200 μl) were loaded onto the IMAC column under appropriate buffer and pH conditions, washed with the equilibration buffer (4 ml) and then eluted with 50 m*M* EDTA–500 m*M* NaCl (5 ml). The non-adsorbed and eluted protein fractions were stored at −15°C immediately after collection. Outcherlony analyses of the protein fractions were carried out with antisera raised against human serum albumin (HSA), immunoglobulin G (IgG), α_2-macroglobulin (α_2-M), transferrin (TrF) and other human proteins as described previously [17,25,28–30].

2.4. Sodium dodecyl sulphate–polyacrylamide gel electrophoresis (SDS–PAGE)

SDS–PAGE of the non-adsorbed and retained protein fractions was performed with a Pharmacia Phast System using 4–15% gradient SDS–PAGE gels and SDS–buffer strips (Pharmacia Biotech). The non-adsorbed and eluted serum protein fractions (200 μl) were prepared by dilution with an equal volume of the electrophoresis buffer, consisting of 500 m*M* Tris–HCl, pH 6.8; Milli-Q water; 10% (w/v) SDS and a few granules of bromophenol. Once diluted, the protein sample were placed in boiling water for 1 min, cooled to room temperature and then stored at −15°C until required. The unfractionated serum protein samples (desalted) were diluted 25-fold with the electrophoresis buffer and analysed as a direct comparison with the fractionated samples. A 12-well applicator (0.3 μl) was used to load the fractionated serum protein samples onto the SDS–PAGE gel while an eight-well applicator (1.0 μl) (Pharmacia Biotech) was used to load the specific standard proteins. The high-molecular-mass standard proteins (Pharmacia Biotech) consisted of thyroglobulin, M_r 669 000; ferritin, 440 000; lactate dehydrogenase, 140 000; and bovine serum albumin, 67 000, whilst the low-molecular-mass protein standards consisted of phosphorylase *b*, M_r 94 000; bovine serum albumin, 67 000; ovalbumin, 43 000; carbonic anhydrase, 30 000; soybean trypsin inhibitor, 20 100 and α-lactalbumin 14 400. The human serum albumin (HSA, fraction V) and transferrin standards were obtained from CSL, and human α_2-macroglobulin was purchased from Sigma. The molecular mass protein standards were diluted in the electrophoresis buffer prior to analysis. Silver staining of the SDS–PAGE gels was performed manually using an adaptation of the automated method reported in the Pharmacia Phast System Electrophoresis manual.

2.5. Chemical reagents and analytical methods

Microanalyses of the chelating ligand were performed by Chemical and Microanalytical Services (CMAS), Melbourne, Australia, while those on the gels were performed by Dairy Technical Services, Melbourne, Australia. Hydrogen-1 nuclear magnetic

resonance (^{1}H NMR) spectra were recorded relative to TMSP at 200 MHz on a Bruker AC 200 spectrometer, whilst carbon-13 nuclear magnetic resonance (^{13}C NMR) spectra were recorded at 50 MHz on a Bruker AC 200 spectrometer or at 75 MHz on a Bruker AM 300 spectrometer. The ^{13}C NMR chemical shifts (δ) are reported in ppm downfield from TMSP. All solvents and reagents were of analytical or reagent grade quality.

2.6. Preparation of sodium N-(2-pyridylmethyl)aminoacetate (carbpyr), ***1***

Redistilled 2-picolylamine, **3**, (5.90 g, 0.055 mol) was placed in a round-bottom flask fitted with a reflux condenser, stirrer bead and dropping funnel. The amine was diluted with an aqueous solution of sodium hydroxide (0.546 g in 5 ml water) and the mixture heated to 60°C. Chloroacetic acid (1.29 g, 0.0136 mol), neutralised with aqueous sodium hydroxide (0.55 g NaOH in 5 ml water), was slowly added to the amine over 1 h. After 8 h, the water was removed under reduced pressure and the solid washed with diethylether (2×50 ml) to remove any remaining amine, **3**. The residual solid was dried by heating under reduced pressure (100°C/660 Pa) over a period of 6 h to give the aminoacetate, **1**, (3.30 g, 95%) as a pale red solid.

^{1}H NMR (200 MHz, ^2H_2O-TMSP): δ 3.22, s, 2H, CH_2-CO; 3.78, s, 2H, CH_2-Ar; 7.23–7.40, m, 2H, 2xArH; 7.73–7.84, m, 1H, ArH; 8.35–8.45, m, 1H, ArH.

^{13}C NMR (50 MHz, ^2H_2O-TMSP): δ 54.17 (CH_2); 55.61 (CH_2); 125.54 (ArCH); 125.72 (ArCH); 140.81 (ArCH); 150.97 (ArCH); 160.24 (quaternary C); 181.78 (–CO–).

2.7. Preparation of N-(2-pyridylmethyl)aminoacetic acid (carbpyr)-Sepharose CL-4B

Suction dried Sepharose CL-4B (2.03 g) was placed into a three-neck round bottom flask fitted with a mechanical stirrer. The gel was suspended in sodium hydroxide (2 *M*, 10 ml) at room temperature for 20 min, then epichlorohydrin (1.6 ml) and sodium borohydride (40 mg) were added. The mixture was left stirring overnight, the gel was then collected by suction filtration and thoroughly washed with water, 30% aqueous ethanol and finally water again. The gel was then returned to the reaction flask, re-suspended in a mixture containing water (8 ml), sodium carbonate (0.5 g) and the aminoacetate, **1**, (1.25 g) and the mixture then heated to 70°C whilst stirring over a period of 24 h. On cooling, the gel was collected by suction filtration and thoroughly washed with water. The nitrogen content of the dry carbpyr-Sepharose CL-4B gel was determined from elemental analysis to be 0.44% (w/w).

3. Results and discussion

3.1. Synthesis of the of immobilised Cu^{2+}–N-(2-pyridylmethyl)aminoacetate-Sepharose CL-4B sorbent

An objective of the present investigation was the preparation of an immobilised IMAC ligate with increased hydrophobic character compared to IDA, but which also had the ability to participate in tridentate coordination interaction with borderline metal ions. Aminopyridine derivatives were chosen not only for their aromaticity, but also for their potential to act as useful N_2O electron donor moieties in IMAC systems. Sodium *N*-(2-pyridylmethyl)aminoacetate, **1**, (Fig. 1) represents a facile alternative for use in IMAC, whereby the pyridyl group replaces one carboxyl group of IDA. With ligand, **1**, the pyridine ring is also substituted at the 2-position leaving a two carbon spacer between the aromatic amine and the aliphatic amine permitting a structurally preferred N_2O square planar bipyrimidal complexation to form with M^{2+} ions, such as Cu^{2+}. The presence of the bulky aromatic ring also constrains the conformational flexibility of the ligand. Immobilisation of this ligand onto the polymer support matrix, through the secondary amine to form a tertiary amine, further reduces the flexibility of the ligand, providing a favourable environment for chelation with M^{n+} ions through entropic restriction effects [17,28], Preparation of the *N*-(2-pyridylmethyl)aminoacetate derivative, **1**, was achieved by alkylating a four-fold molar excess of 2-picolylamine, **3**, with chloroacetic acid in an aqueous sodium hydroxide (Fig. 3). The ^{1}H NMR

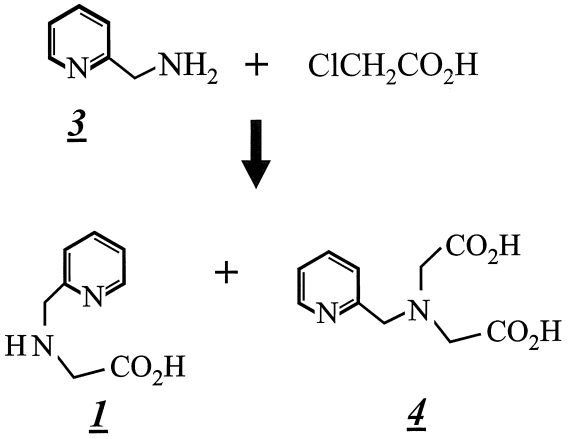

Fig. 3. Synthetic route for the preparation of *N*-(2-pyridylmethyl)aminoacetic acid, **1**.

spectrum of the resulting pale red solid product showed two methylene singlets in the vicinity of δ 3.2 ppm in the ratio of 9:1, consistent with the predominant presence of the desired product, **1,** contaminated with a small amount (ca. 10%) of the dialkylated product, **4**. Thus, the predominant singlet at δ 3.22 ppm apparent in the ^{1}H NMR spectrum of the product can be attributed to the methylene group on the acetate moiety of **1**, whilst the singlet at δ 3.156 ppm can be assigned to the corresponding methylene groups of the corresponding diacetate, **4**. Further purification of the aminoacetate **1** was not necessary since it was considered unlikely that the derivatised tertiary amine, **3**, could react with epoxy groups on the surface of the activated agarose to form a quaternary salt and thus would be removed at the stage of washing the im-carbpyr-Sepharose CL-4B gel.

3.2. Frontal analysis experiments and adsorption behaviour of immobilised Cu^{2+}–N-(2-pyridylmethyl)aminoacetate-Sepharose CL-4B

Frontal analysis of the immobilised Cu^{2+}–*N*-(2-pyridylmethyl)aminoacetate (im-Cu^{2+}–carbpyr)-Sepharose CL-4B matrix was performed with HMYO concentrations ranging from 0.2 to 1.3 mg/ml at a flow-rate of 0.2 ml/min at pH 7.0 and pH 9.0 (Fig. 4A and 4B). The resulting breakthrough curves displayed the typical sigmoidal appearance with the

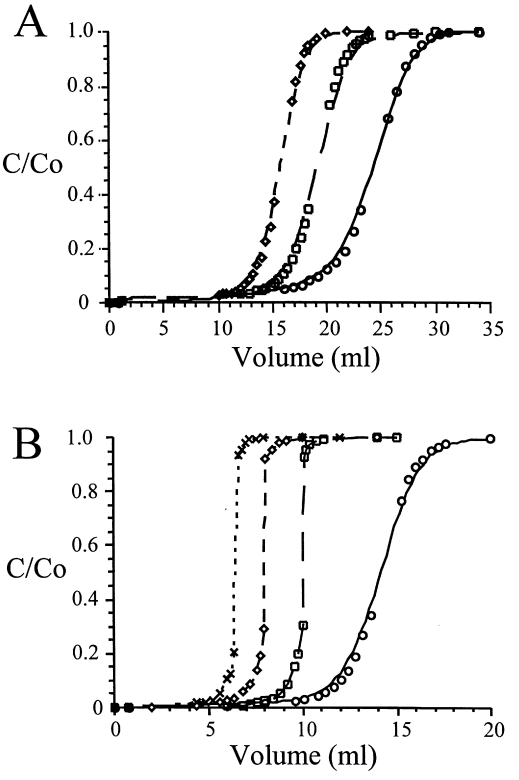

Fig. 4. (A) Representative frontal analysis profile of immobilised Cu^{2+}–*N*-(2-pyridylmethyl)aminoacetate-Sepharose CL-4B sorbent with HMYO concentrations (from right to left) of 0.2, 0.3 and 0.4 mg/ml at pH 7.0. (B) Representative frontal analysis profile of immobilised Cu^{2+}–*N*-(2-pyridylmethyl)aminoacetate-Sepharose CL-4B sorbent with HMYO concentrations (from right to left) of 0.5, 0.8, 1.0 and 1.3 mg/ml at pH 9.0.

breakthrough volume $V_e = 0.5$ progressively decreasing as the concentration of HMYO was increased. In an ideal situation where the rate constant for adsorption is very high, i.e., $k_{on} \rightarrow \infty$ whilst the off rate is very small, i.e., $k_{off} \rightarrow 0$, then the elution front will assume a rectangular breakthrough profile, signifying that no protein was lost before equilibrium was reached. However, due to mass transfer and dispersion effects (associated inter alia with porosity, surface diffusion and surface resistance effects [17,28,29], imperfections in column packing or due to variation in the size of the gel beads making up the packing material, breakthrough curves are usually established as sigmoidal profiles [30]. As HYMO migrates through the IMAC sorbent, the protein interacts with the metal ion through the formation of

Table 1
The adsorption capacity q^* of immobilised Cu^{2+}–*N*-(2-pyridylmethyl)aminoacetate-Sepharose CL-4B sorbent with different HMYO concentrations at pH 7.0 and pH 9.0

Myoglobin (HMYO) (mg/ml)	Mean q^* (±SD)	
	pH=7.0	pH=9.0
0.2	18.11 (±0.01)	21.07 (±0.07)
0.3	21.76 (±0.01)	23.49 (±1.15)
0.4	24.76 (±1.26)	27.04 (±0.63)
0.5	27.76 (±1.35)	28.56 (±0.72)
0.8	29.91 (±0.40)	30.89 (±0.53)
1.0	29.93 (±1.12)	31.15 (±0.58)
1.3	31.04 (±1.32)	31.61 (±0.76)

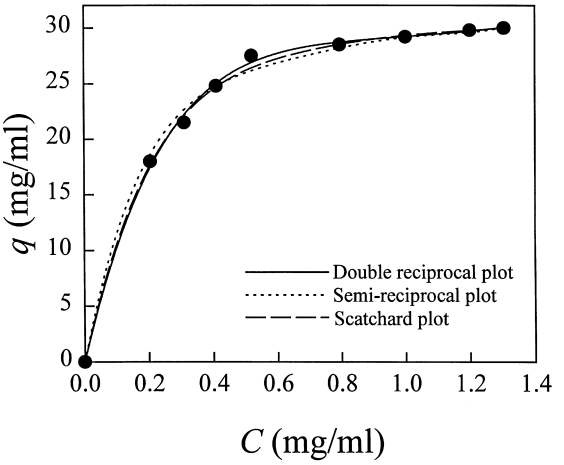

Fig. 5. Adsorption isotherm for the binding of the immobilised Cu^{2+}–*N*-(2-pyridylmethyl)aminoacetate-Sepharose CL-4B sorbent with HMYO concentrations from 0.2 to 1.3 mg/ml at pH 7.0. The simulated isotherm curves based on the K_D values derived from the double reciprocal, semi-reciprocal and Scatchard plots are also included.

coordination bonds between the participating electron rich amino acid residues on the protein, such a histidine, and the electron deficient Cu^{2+} ion. Assuming that a second order rate law and a Langmuirean dependency prevails for the interaction of the immobilised im-Cu^{2+}–carbpyr with HMYO, the amount of protein adsorption (q^*) would be expected to increase as the protein concentration was increases from 0.2 to 1.3 mg/ml. Indeed this pattern was observed (Table 1) with the q_m value reaching a maximal value at a HMYO concentration between 0.8 and 1.0 mg/ml. When the frontal analysis experiments were performed at pH 9.0, similar q_m values were obtained for the adsorption capacity (Tables 1 and 2). However, the dissociation constant K_D of the HYMO–im-Cu^{2+}–carbpyr complex (calculated from the adsorption isotherm) was smaller at pH 9.0 compared to the corresponding value determined at pH 7.0. This reduction in K_D indicates that HYMO is more strongly adsorbed to the im-Cu^{2+}–carbpyr-Sepharose CL-4B sorbent under alkaline buffer conditions.

The adsorption isothermal plot at pH 7.0 (Fig. 5) revealed that the experimental data was in excellent agreement with the calculated isotherms derived from the double reciprocal, semi-reciprocal or Scatchard plot expressions based on a Langmuirean approximation for the interaction with linear dependencies of $1/q$ versus $1/C$, q/C versus q and C/q versus C evident (Fig. 6A–C). The two $1/q$ versus $1/C$ and q/C versus q plots make an interesting comparison because the $1/C$ values in the double-reciprocalplot place a greater emphasis on the lower values of C, whilst the opposite applies with the semi-reciprocal plot where a greater emphasis is placed in the plot on the higher protein concentrations. The outcome of these analyses is that the adsorption isotherms derived from the semi- and double-reciprocal plots are similar but slightly different, resulting in the derivation of slightly different values for q_m and K_D. Significant deviation from linearity in the semi- and double-reciprocal plots, or for that matter the corresponding Scatchard plot, in

Table 2
Maximum adsorption capacity, q_m, and dissociation constant, K_D, for HYMO at pH 7.0 and pH 9.0 with the immobilised Cu^{2+}–*N*-(2-pyridylmethyl)aminoacetate-Sepharose CL-4B sorbent

	Ligand density (μmol/g)	$[Cu^{2+}]$ (μmol/g)	q_m (μmol/g)	K_D (μmol)	$q_m/[Cu^{2+}]$ (·100)
pH=7.0	158	152	1.92	0.0092	1.26
pH=9.0	158	152	1.91	0.0062	1.26

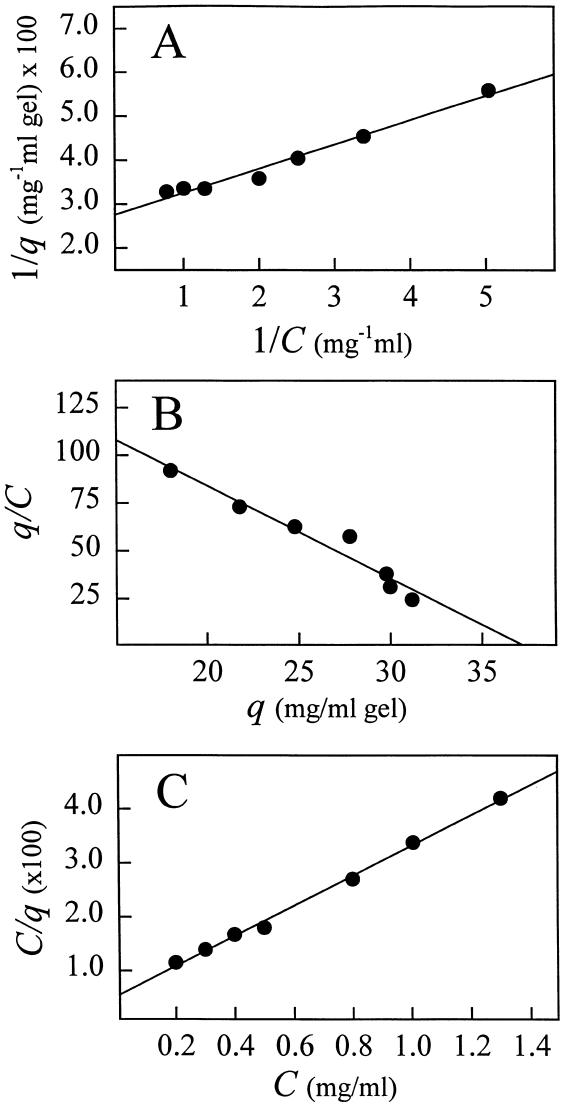

Fig. 6. (A) Double-reciprocal plot for the binding of the immobilised Cu^{2+}–*N*-(2-pyridylmethyl)aminoacetate-Sepharose CL-4B sorbent with HMYO at protein concentrations from 0.2 to 1.3 mg/ml at pH 7.0. (B) Semi-reciprocal plot for the binding of the immobilised Cu^{2+}–*N*-(2-pyridylmethyl)aminoacetate-Sepharose CL-4B sorbent with HMYO at protein concentrations from 0.2 to 1.3 mg/ml at pH 7.0. (C) Scatchard plot for the binding of the immobilised Cu^{2+}–*N*-(2-pyridylmethyl)aminoacetate-Sepharose CL-4B sorbent with HMYO at protein concentrations from 0.2 to 1.3 mg/ml at pH 7.0.

the IMAC of proteins is associated with non-homogeneous interactions, resulting from protein aggregation or dimerisation effects [10] (especially at higher protein concentration) and from non-specific interactions of the protein with the buffer components or with the chromatographic matrix [10,31]. Positive cooperativity in the binding can be revealed as upwardly concaving curves in the Scatchard plots, suggesting the presence or formation of protein species with an increasingly higher affinity for the immobilised metal ion as the protein concentration in solution increases. In contrast, when negative cooperative binding occurs, the presence of species with a lower binding affinity results in the Scatchard plot in downwardly concaving curves [32]. As evident from the Scatchard plot (Fig. 5C), the binding of HMYO to the im-Cu^{2+}–carbpyr-Sepharose CL-4B sorbent can be characterised as following a homogeneous adsorption mechanism with the experimental data clustering around a linear dependency ($r^2=0.9964$) of C/q on C, indicating that the adsorption can be approximated by the independent, homogeneous binding site assumptions implicit to the Langmuirean model.

3.3. Adsorption behaviour with human serum proteins

The im-Cu^{2+}–carbpyr-Sepharose CL-4B sorbent was evaluated for its ability to interact with four proteins present in human serum under acidic, neutral and alkaline conditions. These proteins were HSA (M_r 67 000) which accounts for 47% of the protein content of human plasma [33], TrF (M_r 76 000) [34], IgG (M_r 165 000) [35] and α_2-M (M_r 720 000) [36]. The SDS–PAGE results (Fig. 7) showed that the im-Cu^{2+}–carbpyr-Sepharose CL-6B sorbent bound all four serum proteins at both pH 7.0 and 9.0, but not at pH 5.0. These findings were also confirmed from Ouchterlony immunodiffusion experiments. In a subsequent manuscript, application of IMAC sorbents based on the im-Cu^{2+}–carbpyr ligate for the preparative fractionation of human α_2-macroglobulin and transferrin under step and gradient elution protocols will be described. As noted above, these serum proteins did not bind to the sorbent at pH 5.0, since under these conditions these proteins would be in their protonated state, thereby eliminating the availability of electron donor groups to interact with the immobilised metal ion.

These results with the im-Cu^{2+}–carbpyr-Sepha-

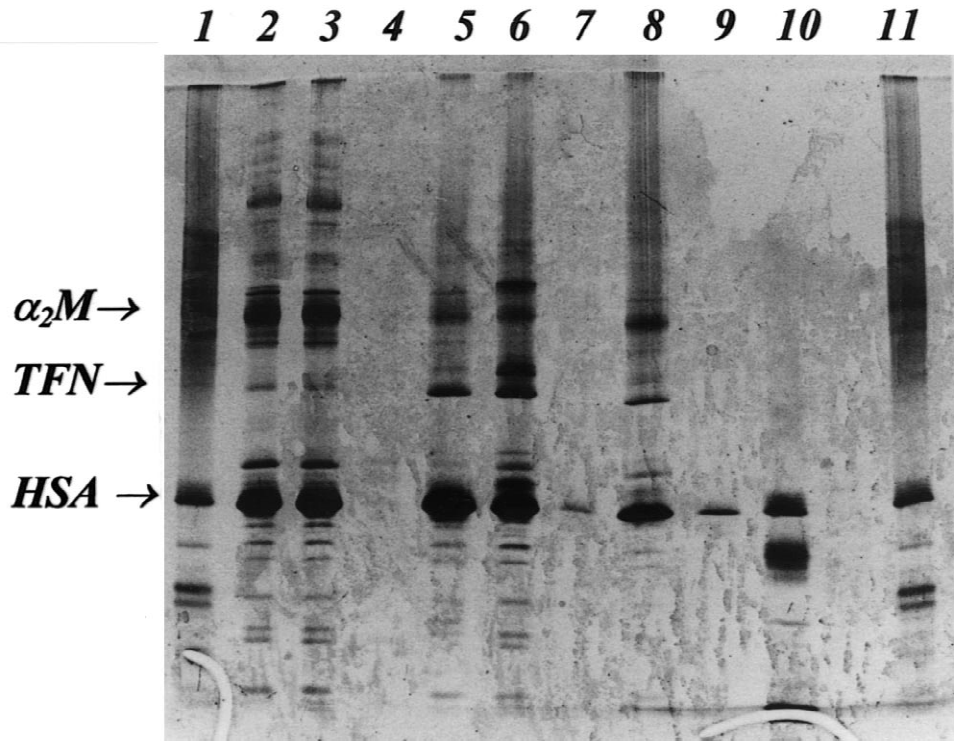

Fig. 7. SDS–PAGE results for the unfractionated and fractionated protein preparations and molecular mass protein standards following the separation of the human serum proteins with the immobilised Cu^{2+}–*N*-(2-pyridylmethyl)aminoacetate-Sepharose CL-4B sorbent. The following samples correspond to the lane positions: lanes 1 and 11, high-molecular-mass standards, thyroglobulin, M_r 669 000; ferritin, 440 000; lactate dehydrogenase, 140 000; bovine serum albumin, 67 000; ovalbumin, 43 000; carbonic anhydrase I, 30 000 and carbonic anhydrase II, 26 000; lanes 2 and 3, unfractionated human serum protein sample; lane 4, adsorbed protein fraction at pH 5.0; lane 5, non-adsorbed protein fraction at pH 5.0; lane 6, adsorbed protein fraction at pH 9.0; lane 7, non-adsorbed protein fraction at pH 9.0; lane 8, adsorbed protein fraction at pH 7.0; lane 9, non-adsorbed protein fraction at pH 7.0; lane 10, low-molecular-mass standards, phosphorylase *b*, M_r 94 000; bovine serum albumin, 67 000; ovalbumin, 43 000; soybean trypsin inhibitor, 20 100 and α-lactalbumin 14 400. The migration position of highly purified samples of human serum albumin (HSA), transferrin (TFN) and α_2-macroglobulin (α_2-M) are also indicated.

rose CL-4B sorbent, although comparable in terms of binding capacities, are dissimilar to those obtained with im-Cu^{2+}–IDA based sorbents [2,7–10] from the perspective of pH optima for binding to the test proteins such as HMYO or HSA. For example, the pH optimum was above pH 7.0 for the im-Cu^{2+}–carbpyr-Sepharose CL-4B sorbent compared to ca. pH 5.5 with im-Cu^{2+}–IDA based sorbents [3,6,10]. Moreover, it can be noted that both IMAC systems show different patterns of elution behaviour with 30 m*M* 2-(*N*-morpholino)ethanesulphonic acid (MES)–30 m*M* imidazole–440 m*M* NaCl–0.005% Brij-35, pH 5.5. These findings suggest that different selectivities can be achieved by exploiting the pH and buffer composition at the loading stage and desorption stages. In the case of the new ligand, **1**, the lone pair of the pyridine nitrogen can participate in the coordination of borderline metal ions such as Cu^{2+}, generating an N_2O donor–acceptor system in contrast to the NO_2 system found with IDA. Despite these differences in their respective Lewis base–Lewis acid characteristics, the immobilised Cu^{2+}–*N*-(2-pyridylmethyl)aminoacetate ligate **1** can still assume a square planar bipyrimidal coordination structure, analogous to that found with immobilised Cu^{2+}–IDA derivatives. This binding behaviour with im-Cu^{2+}–carbpyr-Sepharose CL-4B sorbent for HSA and other proteins at pH values ≥pH 7.0 is

also in contrast to other IMAC sorbent developed in our laboratory [37] based on derivatives of the 2,6-diaminomethylpyridine, **5**, (Fig. 1). IMAC sorbents derived from **5** do not bind to albumin at pH 7.0 and pH 9.0, indicating that the involvement of the pyridine ring substitutions within the ligate plays an important role in determining the binding selectivity with proteins. With the ligate **5**, the orientation of the pyridine moiety can result in Cu^{2+} ion coordinating with an alternative planar face geometry, with the metal ion orientated in the plane of the aromatic ring. From these observations, it can be concluded that the change in the geometry of the ligand–metal ion complex as well as the chemical composition of the ligand per se (the aminoacetate **1** has a carboxyl group, the diaminopyridine **5** does not) can have a significant influence on the selectivity for protein adsorption.

Acknowledgements

We wish to gratefully acknowledge the support of the Australian Research Council. H.C. was a recipient of an Australian PostGraduate Industry Research Award, whilst this work was completed during the tenure of an Alexander von Humboldtforschgspeis to M.T.W.H.

References

[1] E. Sulkowski, Trends Biotechnol. 3 (1985) 1.
[2] L. Kagedal, in: J.C. Janson, L. Ryden (Eds.), Protein Purification, VCH, Weinheim, 1989, pp. 227–251.
[3] M. Zachariou, M.T.W. Hearn, Biochemistry 35 (1996) 202–211.
[4] W. Jiang, M.T.W. Hearn, Anal. Biochem. 242 (1996) 45–54.
[5] J.W. Wong, R.L. Albright, N.H.L. Wang, Sep. Purif. Methods, 20 (1991) 49.
[6] M. Zachariou, I. Traverso, L. Spiccia, M.T.W. Hearn, J. Phys. Chem., 100 (1995) 12680–12690.
[7] J. Porath, I. Carlsson, I. Olsson, G. Belfrage, Nature 258 (1975) 598–599.
[8] J. Porath, B. Olin, Biochemistry 22 (1983) 1621–1627.
[9] J. Porath, P. Hansen, J. Chromatogr. 550 (1991) 751–758.
[10] Z. El Rassi, C. Horvath, in: K.M. Gooding, F.E. Regnier (Eds.), HPLC of Biological Macromolecules, Marcel Dekker, New York, 1990, pp. 179–213.
[11] U. Zawistowska, K. Sangster, J. Zawistowski, J. Langstaff, A.D. Friessen, Cereal Chem. 65 (1988) 5413–5419.
[12] K.M. Weeransinghe, M.F. Scully, V.V. Kadder, Biochim. Biophys. Acta 839 (1985) 57–71.
[13] S. Otsuka, T. Yamanaka (Eds.), Bioactive Molecules, Kodansha, Tokyo, 1988, pp. 18–45.
[14] R. Mathur, K. Panneerselvam, A.S. Balasubramanian, Biochem. J. 253 (1988) 677.
[15] J. Porath, Trends Anal. Chem. 7 (1988) 254–257.
[16] T. Mantovaara, H. Pertofz, J. Porath, Biotechnol. Appl. Biochem. 11 (1989) 564–572.
[17] H. Chaouk, S. Middleton, W.R. Jackson, M.T.W. Hearn, Int. J. BioChromatogr. 2 (1997) 153–190.
[18] E. Hochuli, W. Bannwarth, H. Döbeli, D. Stuber, Bio/Technology 6 (1988) 1321–1324.
[19] K.R. Sticha, C.A. Sieg, C.P. Bergstrom, P.E. Hanna, C.R. Wagner, Protein Expression Purif. 10 (1997) 141–153.
[20] N. Fan, K.B. Rank, J.W. Leone, R.L. Heinrikson, C.A. Bannow, C.W. Smith, D.B. Evans, S.M. Poppe, W.G. Tarpley, D.J. Rothrock, A.G. Tomasselli, K.M. Sharma, J. Biol. Chem. 270 (1995) 13573–13579.
[21] N. Ramadan, J. Porath, J. Chromatogr. 321 (1985) 105–113.
[22] M. Zachariou, M.T.W. Hearn, J. Chromatogr. 599 (1992) 171–177.
[23] M. Zachariou, I. Traverso, M.T.W. Hearn, J. Chromatogr. 646 (1993) 107.
[24] J. Porath, Protein Expression Purif. 3 (1992) 263–281.
[25] W. Jiang, B. Graham, L. Spiccia, M.T.W. Hearn, Anal. Biochem. 255 (1997) 47–58.
[26] L.W. Nichol, A.G. Ogston, D.J. Winzor, W.H. Sawyer, Biochem. J. 143 (1974) 435–447.
[27] F.B. Anspach, A. Johnston, H.J. Wirth, K.K. Unger, M.T.W. Hearn, J. Chromatogr. 476 (1989) 205–217.
[28] F.B. Anspach, A. Johnston, H.J. Wirth, K.K. Unger, M.T.W. Hearn, J. Chromatogr. 499 (1990) 103–121.
[29] H.J. Wirth, K.K. Unger, M.T.W. Hearn, Anal. Biochem. 208 (1993) 16–25.
[30] M. Belew, T.T. Yip, L. Andersson, J. Porath, J. Chromatogr. 403 (1987) 403–410.
[31] R. Blanco, A. Arai, N. Grinberg, D.M. Yarmush, B.L. Karger, J. Chromatogr. 482 (1989) 1–15.
[32] F.W. Dahlquist, Methods Enzymol. 48 (1978) 270–295.
[33] W.G.M. Braam, in: On the Structure of the Albumin Molecule, Offsetdrukkerij Faculteit der Wiskunde en Natuurwetenschappen, Nijmegen, 1972, pp. 1 and 76.
[34] P. Saltman, C. Billups, L. Pape, J. Biol. Chem. 242 (1967) 4289–4296.
[35] J.R. Clamp, I. Johnson, in: A. Gottschalk (Ed.), Glycoproteins – Their Composition, Structure and Function, Elsevier, Amsterdam, 1972, pp. 612–652.
[36] R. Bourillon, E. Razafimahaleo, in: A. Gottschalk (Ed.), Glycoproteins – Their Composition, Structure and Function, Elsevier, Amsterdam, 1972, pp. 699–716.
[37] H. Chaouk, M.T.W. Hearn, J. Biochem. Biophys. Methods (1999) in press.